Journal of Molecular Liquids 163 (2011) 64–69

Contents lists available at SciVerse ScienceDirect

Journal of Molecular Liquids

journal homepage: www.elsevier.com/locate/molliq

Ionic liquids at the air/water interface

Esteban Clavero [a], Javier Rodriguez [b,c,*]

[a] Centro de Estudios e Investigaciones, Universidad Nacional de Quilmes, Sáenz Peña, 352, 1876, Bernal, Argentina
[b] Departamento de Física, Comisión Nacional de Energía Atómica, Avenida Libertador, 8250, 1429, Buenos Aires, Argentina
[c] ECyT, UNSAM, Martín de Irigoyen 3100, 1650, San Martín, Provincia de Buenos, Aires, Argentina

ARTICLE INFO

Article history:
Received 5 March 2011
Received in revised form 18 July 2011
Accepted 20 July 2011
Available online 23 August 2011

Keywords:
Ionic liquids
Molecular dynamics
Surface activity

ABSTRACT

We present molecular dynamics experiments of Langmuir monolayers of iodide and chloride salts of 1-octyl-3-methylimidazolium adsorbed at water/air interfaces, covering a concentration range that spans from a dilute regime up to the experimental surface saturation for both systems. For the chloride case we observed a propensity to form monolayers with nearly equal surface concentration of both cations and anions; whereas for the iodide system, the more marked propensity to surface solvation of the anionic species leads to the appearance of quasi-double-layered structures. At the surface, the imidazolium rings remain in contact with the aqueous substrate, with a wide variety of orientations with respect to the surface normal direction. The global tilt of the hydrophobic tail of the cations was found to be $\theta_{tl} \sim 40°$ and 50°, for the chloride and iodide salts, respectively. Polarization fluctuations of the interface are analyzed in terms of those describing charge distributions of the adsorbed species and the electrical response of the solvent as well. The characteristics of the local densities for the ionic species at the interface provide arguments for the microscopic interpretation of the differences observed in scattering experiments on the dependence of the surface tension with the surfactant concentration.

© 2011 Elsevier B.V. All rights reserved.

1. Introduction

Room temperature ionic liquids (RTIL) are molten salts with normal boiling points close or below ambient conditions. They have important practical applications in many chemical processes, most notably, those derived from their ability to host a large variety of polar and non-polar solutes. [1–5] The interest in the use of these liquid phases derives from several chemically appealing characteristics, such as minimal volatility, high thermal stability and viscosity and the wide versatility to choose "tailored" anion–cation mixtures.

Experimental and theoretical researches on RTIL have experienced a marked increment in recent years[6]. The corresponding studies include isotropic macroscopic phases [7–14] and also inhomogeneous environments, such as liquid/liquid and liquid/air interfaces[15–33]. Focusing in the latter systems, and despite of the large body of research available, there are still several important questions pertaining to the surface activity of RTIL that await proper elucidation. For example, one intriguing observation has been recently reported in a paper by Bowers et al. [22]. Using small-angle neutron scattering techniques, Bowers analyzed Langmuir monolayers of ionic liquids based on the 1-alkyl-3-methylimidazolium cation adsorbed at the water/air interface. Contrary to what is usually reported for common surfactants, the dependence of the surface tension of monolayers comprising 1-octyl-3-methylimidazolium iodide [C_8mim][Cl] versus the global concentration of the RTIL exhibits a minimum near the critical micellar concentration (cmc = 100 mmol dm^{-3}). In contrast, the surface tension of interfaces hosting the related RTIL [C_8mim][I], shows the usual behavior, characterized by a sharp drop for $c \lesssim$ cmc, followed by a flat profile beyond this critical concentration.

Subsequent investigations performed by Sung et al. [24] showed that the peculiar behavior observed by Bowers for the surface tension of [C_8mim][Cl] monolayers was also found in those comprising the shorter-chain RTIL 1-butyl-3-methylimidazolium tetrafluoroborate [C_4mim][BF_4]. As a plausible explanation of the "unexpected," non-monotonic behavior, the authors have speculated on the possibility that important surface structural modifications at the surface might occur beyond the cmc. According to Sung et al. [24], in this concentration regime, the energetics of the interface – originally dictated by interactions involving the organic tails – would be closer to that exhibited by interfaces of aqueous electrolytes, where ionic forces prevail. In a similar context, Picálek et al. [32] have recently reported molecular dynamics experiments on bulk and surface phases of [C_4mim][BF_4]-water and [C_4mim][PF_6]-water solutions at a series of solute concentrations, ranging from pure water up to the corresponding cmc. Their surface tension results, although rather noisy, provide clues that would suggest that the above justification – i.e. a net increase of the local concentration of anionic species – is physically sound. Motivated by these observations, in the present paper, we return to the analysis of the longer chain RTIL originally investigated by Bowers et al. using molecular dynamics experiments. Our objective

* Corresponding author at: Departamento de Física, Comisión Nacional de Energía Atómica, Avenida Libertador, 8250, 1429, Buenos Aires, Argentina.
E-mail address: jrodrigu@tandar.cnea.gov.ar (J. Rodriguez).

0167-7322/$ – see front matter © 2011 Elsevier B.V. All rights reserved.
doi:10.1016/j.molliq.2011.07.014

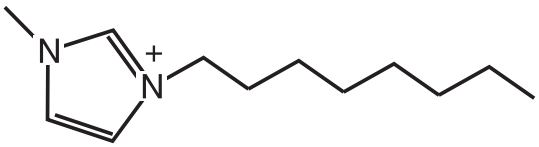

Fig. 1. Chemical structure of 1-octyl-3-methylimidazolium cation.

was to establish differences in the equilibrium solvation structures of the adsorbed monolayers at the vicinity of the cmc that, in turn, would provide additional clues to validate the previous mentioned hypothesis.

2. Model

The results presented in this paper correspond to molecular dynamics experiments performed on aqueous slabs containing $N_w = 800$ molecules. The samples were obtained from fully periodic systems, confined within a rectangular box, with linear dimensions 31.17 Å × 31.17 Å × 24.95 Å. After an initial equilibration period of ~200 ps at $T = 298.15$ K and $p = 1$ bar, periodic boundary conditions were suppressed along the z-axis. In addition, equal numbers N_α of 1-octyl-3-methylimidazolium [C_8mim] cations (see Fig. 1) and simple anions such as Cl^- and I^-, were distributed in the vicinity of one of the free surfaces of the slabs, in a random fashion. In what follows, systems with Cl^- and I^- will be referred to as of type A and B, respectively. The initial intramolecular configurations of the octyl chains in the [C_8mim] corresponded to fully *trans* conformers, with their head-to-tail vectors aligned parallel to the z-direction. For each system three different number of RTIL ion pairs were placed at the surface of the water substrate in that way. These amounts were chosen in order to obtain surface concentrations that roughly correspond to 0.5, 1.0 and 1.5 times those experimentally reported for the corresponding saturated monolayers: $\Gamma_A = 1.3 \times 10^{-2}$ Å^{-2} and $\Gamma_B = 8.5 \times 10^{-2}$ Å^{-2}[22]. It is important to remark that our objective was focused in reproducing the reported surface excesses corresponding to different bulk concentrations at the vicinity of the cmc. In doing so, no efforts were made in analyzing the characteristics and the eventual influence of the bulk states on the surface states of the RTIL.

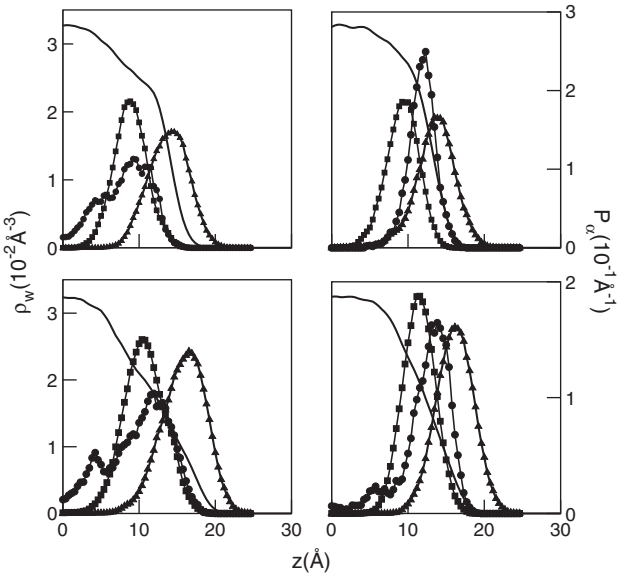

Fig. 2. Water local density (solid line, left axis) and probability densities (solid line, right axis) for the [C_8mim][Cl] (left panels) and the [C_8mim][I] (right panels). The upper panels correspond to the lower concentrations analyzed; whereas the lower panels show results from the higher concentrations. For the sake of clarity, results for the intermediate concentrations are not shown. Tail and head distributions are shown with black squares and triangles, respectively. The anion distribution is presented with black circles.

The Hamiltonian employed corresponded to the classical, non-additive, polarizable, RPOL model developed by Dang[34]. In addition to the direct interactions between partial charges, Coulomb forces in Dang's model also include interactions involving induced dipoles, centered at the positions of the atomic sites. Length, energy and polarization parameters for interactions involving anionic species were taken from Ref. [35]. Interactions involving the cationic species were modeled using the GROMACS force field[36–38]. For these species, polarization effects were not taken into account, since previous simulation studies have shown that the explicit incorporation of such fluctuations in these molecules can be safely disregarded at least, in what to its structural behavior concerns. A detailed analysis of the relevance of the incorporation of polarization of cations and anions to the force field for the determination of dynamical and equilibrium properties of ionic liquids can be found in Refs. [39] and [40].

The simulation experiments corresponded to microcanonical runs performed at a temperature close to $T = 298$ K. Statistical averages were collected from trajectories lasting typically ~3 ns. Long-range Coulomb interactions were treated using Ewald sums specially adapted for systems with a slab geometry and include interactions between partial charges and induced dipoles[41,42]. For additional technical details pertaining to our simulation procedure, we refer the interested reader to Ref. [43].

3. Results

The first aspect that we will address concerns the structure of the aqueous interfaces. Results for the water local density profiles,

$$\rho_w(z) = \frac{1}{A}\left\langle \sum_{i=1}^{N_w} \delta(Z_i - Z_{CM} - z) \right\rangle \quad (1)$$

for both systems, are shown in the four panels of Fig. 2. In the previous equation, the angular brackets denote an equilibrium ensemble average, whereas Z_i and Z_{CM} refer to the z-coordinates of the i-th water oxygen and the center of mass of the water slab, respectively. In Eq. (1), $\rho_w(z)dz$ represents the number of water molecules per unit of area, A, at the xy-plane, with their oxygen sites lying between z and $z + dz$.

The corresponding density profiles look rather asymmetric, so we estimated the position of the Gibbs dividing surfaces ($\bar{z}_G$) and the corresponding interface widths (Δz) by adopting the usual criterion based on the positions of the 10% and 90% of the bulk density. The results for these magnitudes appear in Table 1a and reveal that the localizations of the interfaces remain practically unchanged, regardless of the system, or concentration, considered. The corresponding widths are somewhat narrower for systems of type B, while polarization fluctuations do not modify the geometrical characteristics of the aqueous interface in a sensible fashion either. A comparison between the overall interface widths in the presence of the RTIL monolayers and in those hosting a prototype cationic surfactant, say tetradecyltrimethylamonium bromide, shows comparable scenarios. [44,45].

For the rest of the species, we computed site probability distributions of the type:

$$P_\alpha \propto \left\langle \sum_i \delta(z_i^\alpha - Z_{CM} - z) \right\rangle; \quad (2)$$

where z_i^α refers to the z-coordinate of site α in the i-th molecule. The anionic distributions look both asymmetric and differ at a quantitative level. Interestingly, these distributions can be reasonably well

Table 1

a. Structural parameters for the aqueous interface

System	N_{IL}	$\hat{z}_G$	Δz	$\mathcal{P}_{ILC}$	$\mathcal{P}_{ILA}$
A	8	12.36	10.18	0.06	0.08
	13	12.19	11.00	0.20	0.27
	18	12.17	12.53	0.30	0.32
B	4	12.40	7.07	0.07	0.40
	8	12.37	9.41	0.17	0.51
	12	12.27	9.21	0.35	0.60

b. Anion surface solvation parameters

System	N_{IL}	δ_α^{out} (Å)	δ_α^{in} (Å)	σ_α^{out} (Å)	σ_α^{in} (Å)
A	8	−1.79[a]	−0.65[a]	6.29	11.32
	13	−0.46[a]	−5.4[a]	6.3	11.2
	18	−1.56[a]	−6.42[a]	6.67	14.20
B	4	0.47[a]	−0.69[a]	3.43	5.65
	8	0.75[a]	−4.40[a]	5.00	12.20
	13	1.38[a]	−3.88[a]	5.53	11.33

c. Cation surface solvation parameters

System	N_{IL}	δ_{IR} (Å)	δ_{HT} (Å)	$\langle cos\theta_{tl}\rangle$	$\langle r_{tl}\rangle$ (Å)
A	8	−3.36[a]	1.76[a]	0.74	9.72
	13	−1.98[a]	3.11[a]	0.75	9.94
	18	−1.31[a]	4.13[a]	0.77	9.81
B	4	−2.95[a]	1.43[a]	0.62	9.59
	8	−2.14[a]	2.58[a]	0.69	9.95
	12	−0.82[a]	3.91[a]	0.69	9.67

[a] Computed from $\delta_\alpha = \bar{z}_\alpha - \bar{z}_G$ (see text).

described as linear combinations of two adjacent, Gaussian-like profiles of the type:

$$P_\alpha^i(z) \propto exp\left[-\frac{4\left(z-\bar{z}_\alpha^i\right)^2}{\left(\sigma_\alpha^i\right)^2}\right]; \tag{3}$$

centered at inner and outer surface slabs, where $\alpha = Cl^-$, I^- and $i =$ in, out. The last distributions shown in Fig. 2 correspond to the centers of mass of the imidazolium rings (IR) and for the 8 saturated carbon groups comprising the hydrophobic tails (HT) of the [C_8mim]. For the latter species, the corresponding profiles look practically Gaussian.

Table 1b and c summarizes results for the geometrical parameters describing the distributions. Leaving aside for the moment the obvious differences in the global concentrations, the shifts in the positions of the distribution maxima ($\delta_\alpha = z_\alpha^{max} - \bar{z}_G$ for $\alpha = I^-$ and Cl^-, respectively), reveal a more marked propensity of the anionic species to exhibit surface states, when compared to the imidazolium rings localization. Moreover, if a comparison is established between the two anions, I^- atoms clearly show a stronger tendency to occupy outer positions, most likely due to their bigger overall size. Both facts are accordant with recent simulation results. [46,47].

To get an idea of the excess surface concentration of the different species, we computed cumulative integrals of the type:

$$\mathcal{P}_\alpha = \int_{\bar{z}_G}^{\infty} P_\alpha(z')\mathrm{d}z' \tag{4}$$

where $\alpha =$ ILC, ILA refers to cationic heads and anionic counterions of the RTIL, respectively. Note that $\mathcal{P}_\alpha$ represents the fraction of species α lying beyond the Gibbs dividing surface (see results listed in columns 5 and 6 of Table 1a). The analysis of the variation of the different $\mathcal{P}_\alpha$ as a function of the global RTIL concentration leads to the following conclusions: (i) as expected, the surface concentration of RTIL increases with the increment of its total concentration; (ii) for system of type A, the surface distribution of ionic species seems to be balanced, i.e. ILA and ILC surface concentrations do not differ in a significant way; (iii) on the other hand, in system of type B, the ILA shows a more marked tendency to occupy surface states, than the corresponding cations, even at the highest concentration regime analyzed.

The combination of the hydrophobic interactions with the substrate and the tail–tail coupling dictate the main features characterizing the solvation of octyl chains at the interfaces. To characterize the latter solvation, we focused attention on two parameters: (i) the first one concerned the overall intramolecular configuration expressed in terms of r_{tl}, the average distance between the more distal CH_3 group and the center of mass of the IR; (ii) the second one was related with the tail tilt, $cos\theta_{tl}$, expressed in terms of the projection of the head-to-tail vector along the z-axis. Results for these two magnitudes are listed in the 5th and 6th columns of Table 1c. Note that, in all cases, the geometrical arrangement of the hydrophobic tails can be pictured as elongated structures, with little variations in the original intramolecular configurations ($r_{tl} = 11$ Å for a fully *trans* conformer) and with a global tilt close to $\theta_{tl} = 40°$ and $\theta_{tl} = 50°$, for the A and B systems, respectively. This difference could be rationalized in terms of the larger intermolecular distances between IR in systems of type B (due to the bigger size of the surface anion I^-) that, in turn, would allow for wider displacements of the terminal methyl groups towards the water substrate. Concerning the orientations of the imidazolium rings, in the vast majority of the configurations, we observed that the planes of the IR remained in contact with the water substrate, giving rise to a wide variety of ring orientations, due the high irregularity of the underlying interface.

We will now analyze the characteristics of the surface electric fields and the orientational correlations of the water substrate that are induced by the charge density of the adsorbed RTIL. We start by analyzing results for:

$$\rho_q(z) = \frac{1}{A}\left\langle \sum_{\alpha,i} q_\alpha \delta(z_i^\alpha - z)\right\rangle; \tag{5}$$

in the previous equation, the sum includes exclusively the charges of the ionic species. Profiles for $\rho_q(z)$ are depicted in the top and bottom panels of Fig. 2 for systems of type A and B, respectively. The profiles for the two RTIL analyzed differ at a qualitative level: for systems of type A, the charge distributions exhibit two regions: (i) a $z<6$ Å, inner zone, where the charge density is negative, due to the prevalence of solvated Cl^- ions, followed by a (ii) $z>6$ Å, outer, positively charged region, which hosts the hydrophobic cationic species. For charge distributions of RTIL of type B, the previous scenario is reversed; due to the larger surface activity of the anions, the outer region is now the one that is negatively charged. In addition, in the latter case, the boundary between these regions moves from $z = 10$ Å out to $z = 12.5$ Å as the concentration increases. As a side comment, we note that at the largest RTIL concentration examined, a minor fraction of the anions was found to move deeper into the central portion of the slab, which gives rise to a third, negatively charged, internal ($z<7$ Å) region. From the charge densities, it is possible to estimate the surface charge density of regions located at the vicinity of the Gibbs dividing surface:

$$\sigma_\alpha^{in} = \int_{\bar{z}_G - \frac{\Delta z}{2}}^{\bar{z}_G} \rho_q^\alpha(z')\mathrm{d}z', \qquad \sigma^{\alpha out} = \int_{\bar{z}_G}^{\bar{z}_G + \frac{\Delta z}{2}} \rho_q^\alpha(z')\mathrm{d}z', \tag{6}$$

with $\alpha =$ A and B. The analysis of the values of σ_α listed in Table 2 reveals: (i) the existence of a subtle, σ^{out} positive surface excess charge in systems of type A; (ii) in contrast, σ_B^{out} is approximately one order of magnitude bigger than, and opposite in sign, with respect to

Table 2
Surface charge density of the Gibbs dividing surface boundary regions.

System	N_{IL}	σ^{in} (10^{-4} e Å^{-2})	σ^{out} (10^{-4} e Å^{-2})
A	8	14.1	1.9
	13	27.3	2.0
	18	34.0	7.0
B	4	2.8	−11.0
	8	18.7	−22.0
	12	34.7	−26.0

σ_A^{out}; (iii) for the case of the inner boundaries, the values of σ^{in} are, for both systems, of the same order of magnitude, and correspond to positive excess charge in all cases. Note that these features are accordant with the structural analysis described in previous paragraphs. It is well known that departures from the electric surface neutrality normally promote a reduction in the surface tension (γ) of Hg-electrolyte solutions interfaces[48]. Moreover, the extent of the observed reduction is proportional to the excess surface charge. Following this line of reasoning, and taking into account the reported experimental trends for γ, [22] we are led to conclude that the differences between the surface tensions of systems of type A and B are determined to a large extent by the Coulomb imbalance at the interface, with much minor contributions arising from interactions involving the hydrophobic tails.

Complementary information about the electrical characteristics of the different interfaces can be obtained from the analysis of the $P_{cos\theta_w}(z)$, the orientational distribution of the water substrate:

$$P_{cos\theta_w}(z) = \frac{1}{A}\left\langle \sum_i^{N_w} \frac{\mu_i \cdot \hat{z}}{|\mu_i|}\delta\left(z_i^O - Z_{CM} - z\right)\right\rangle \quad (7)$$

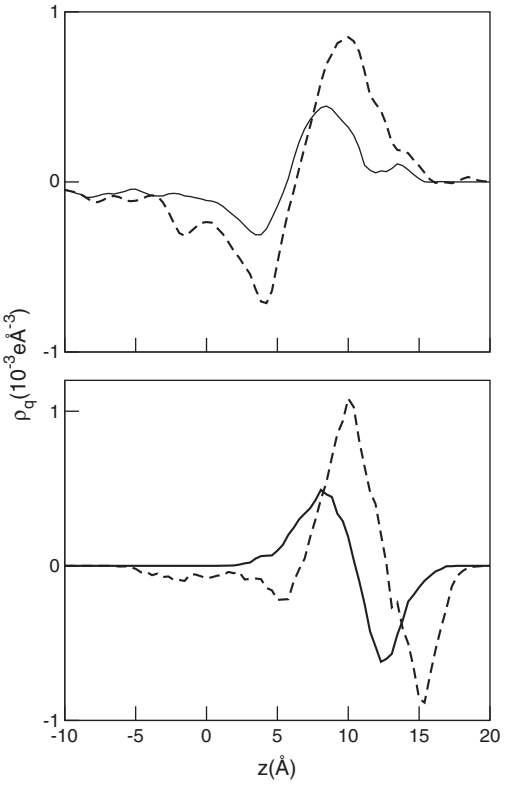

Fig. 3. Charge density for the ionic species. Top panel: system A. Bottom panel: system B. Solid (dashed) lines correspond to the lower (higher) concentrations analyzed. Results for the intermediate concentrations are not shown.

where μ_i represent the permanent dipole of the i-th water molecule and $\hat{z}$ represents a unit vector along the z-direction.

Previously, we reported that, in passing from the bulk to the surface of the slab, the RTIL charge spatial correlations show an inner diffuse anionic layer (most notably in the case of system A and only perceptible for system B at the more concentrated regime). This region is followed by an external cationic layer, in close contact with the internal boundary of the interface. These characteristics promotes modifications of the orientational response of the water molecules that participate in the solvation of the RTIL. The overall shape of the plots for $P_{cos\theta}(z)$ shown in the top panel of Fig. 4 (type A) is dominated by the antiparallel branch (i.e. $\mu_i \cdot \hat{z} < 0$) which extends deep into the bulk zone. In addition, one also observes a much more reduced, positive contribution starting approximately at the location of the Gibbs dividing surface, which would correspond to water molecule lying beyond the position of the positive imidazolium rings. The characteristics of the profiles of $P_{cos\theta_w}(z)$ for systems of type B (bottom panel) are strongly dependent on the overall RTIL concentration and can be interpreted by the simple inspection of the profiles of $\rho_q(z)$ shown in Fig. 3. At low coverage, the alternation of positive and negative excess charge gives rise to a net parallel alignment of the water dipoles. On the other hand, the sequence of negative–positive–negative excess charges found at higher concentrations gives rise to a strong antiparallel–parallel sequence in the plot of $P_{cos\theta_w}(z)$ (dashed line).

The last topic of our analysis involved the examination of spatial correlations between adsorbed species. For that purpose, we found it convenient to analyze two dimensional correlations of the type:

$$g_{\alpha\gamma}(r) = \frac{A}{N_\alpha N_\gamma 2\pi r}\sum_{i'}^{N_\alpha}\sum_{j'}^{N_\gamma}\left\langle \delta\left(|\mathbf{r}_{i'}^{\alpha} - \mathbf{r}_{j'}^{\gamma}| - r\right)\right\rangle. \quad (8)$$

where the primed indexes correspond to those sites comprising both cations and anions of the RTIL, lying at the interface. The results are

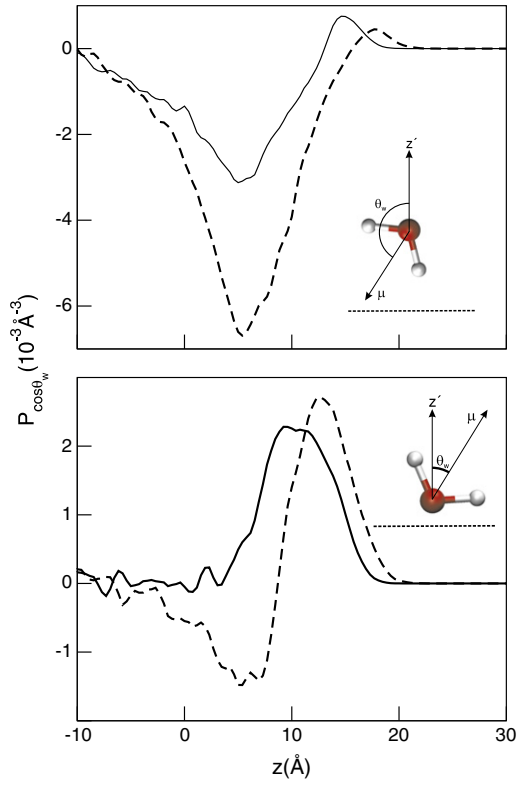

Fig. 4. Orientational distribution of the water substrate. Same references as in Fig. 3.

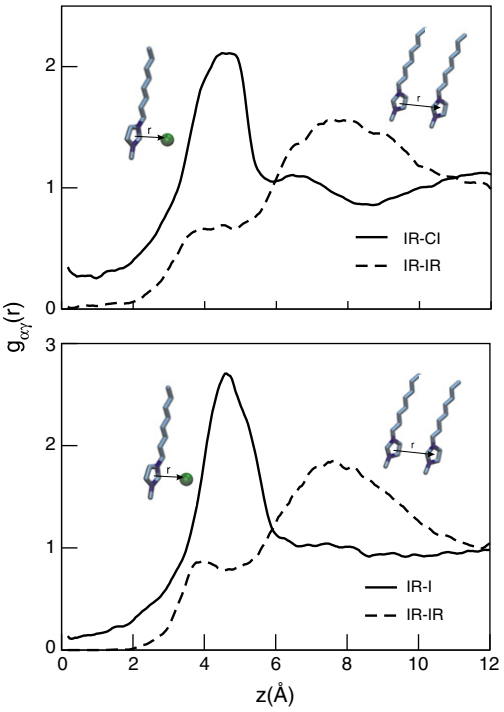

Fig. 5. Two dimensional pair correlation functions between the ionic species: g_{IR-IR} (dashed lines), g_{IR-X} (solid lines). Top panel: systems of type A (X = Cl^-); bottom panel: systems of type B (X = I^-). Both figures correspond to the intermediate concentration analyzed for both systems.

shown in Fig. 5. In both cases, correlations between the centers of mass of the IR are characterized by a first peak centered at $r = 4$ Å followed by a much broader one, located at $r = 7.5$ Å. This feature is consistent with the spatial correlations found in aqueous [C_8mim][NO_3] by Jiang et al. [49].The direct inspection of a large number of configurations shed light on the spatial characteristics associated to these two peaks: the ones located at $r = 4$ Å suggest a parallel stacking of contact-pair imidazolium rings, whereas the much broader second peaks at $r = 7$ Å correspond to an indirect "bridging" coordination of IR by anionic species of the type IR···X^-···IR.

4. Concluding remarks

In this article, we have presented molecular dynamics simulation results pertaining to the surfactant properties of two ionic liquids comprising simple anionic species and 1-octy-3-methylimidazolium adsorbed at air–water interfaces. Consequently, our analysis focused exclusively on the characteristics of the solvation of surface states; in this respect, the eventual presence of a bulk phase in equilibrium was only taken into account as a controlling agent of the effective surface density.

The main conclusions of the paper can be summarized as follows: (i) We have confirmed that I^- anions show a more marked propensity to exhibit surface states than Cl^- ones. (ii) Concerning the characteristics of the surface solvation of the cations, the imidazolium groups lie somewhat deeper into the aqueous substrate than the rest of the charged species, whereas the overall structure of the hydrophobic portions of the groups can be pictured in terms of elongated segments, with global tilts close to $\theta_{tl} = 40°–50°$, depending on the counterion considered. (iii) The spatial correlations in the vicinity of the IR are accordant with parallel stacking of IR-contact-pairs at short distances and indirect "bridged" structures of the type IR···X^-···IR. (iv) The ionic contributions to the total charge density at the surface differ considerably when the scenarios of the two adsorbed ionic liquids are compared. In particular, for [C_8mim][Cl] monolayers, the overall profile along the direction normal to the surface suggests the existence of a surface structure comprising a electrically neutral anion/cation mixture followed by an internal region where the imidazolium rings prevail. Deeper within the substrate, the latter layer is followed by a much more diffuse one that includes the rest of the Cl^- ions. On the other hand, the propensity of the I^- anions to lie at the outermost portion of the interface hosting [C_8mim][I], leads to an interface structure, characterized by an ionic double layer, in which the anions occupy more external positions. (v) We tend to believe that the presence of the negative inner layer found for [C_8mim][Cl] could be considered as a source of additional charge available to be hosted at the interface, beyond the cmc. Further neutralization of the positive excess charge (associated to the imidazolium rings located at the inner boundary of the interface) would, in turn, lead to an increment in γ, corroborating the physical interpretation provided by Sung et al. [24]. Of course, a more conclusive response to this puzzling result would be the computation of the surface tension at and beyond the cmc value. It is well documented that, due to the slow convergence of the equilibrium averages, the uncertainties associated to the predictions of this magnitude are usually non-negligible. For example, even in simple cases such as aqueous solutions of different sodium halides, relative errors associated to the surface tensions after long simulation runs (of the order of 0.1 μs) remain in the order of ~20% [33,50]. Such limitation precluded us to obtain physically meaningful values for the surface tension, results that could be directly contrasted to experimental measurements [22]. We believe that the results presented here provide new and interesting insights to rationalize the complex thermodynamic behavior of Langmuir monolayers comprising sparingly soluble RTIL in aqueous solutions.

Acknowledgments

We thank Daniel Laria for many illuminating discussions and valuable suggestions, and for thoroughly reading this manuscript. J.R. is a staff member of CONICET (Argentina).

References

[1] J.F. Wishart, E.W. Castner, The Journal of Physical Chemistry. B 111 (2007) 4639.
[2] P. Wasserscheid, Nature 439 (2006) 797.
[3] T. Welton, Chemical Reviews 99 (1999) 2071.
[4] R.D. Rogers, K.R. Seddon, Science 302 (2003) 792.
[5] W. Hermann, Angewandte Chemie, International Edition 47 (2008) 654.
[6] G.A. Voth, Accounts of Chemical Research 40 (2007) 1077.
[7] S. Hayashi, R. Ozawa, H. Hamaguchi, Chemistry Letters 32 (2003) 498.
[8] A. Mele, G. Romano, M. Giannone, E. Ragg, G. Fronza, G. Raos, V. Marcon, Angewandte Chemie 45 (2006) 1123.
[9] J.G. Huddleston, A.E. Visser, W.M. Reichert, H.D. Willauer, G.A. Broker, R.D. Rogers, Green Chemistry 3 (2001) 156.
[10] H. Tokuda, K. Hayamizu, K. Ishii, M.A.B.H. Susan, M. Watanabe, The Journal of Physical Chemistry. B 109 (2005) 6103.
[11] H. Tokuda, K. Ishii, M.A.B.H. Susan, S. Tsuzuki, K. Hayamizu, M. Watanabe, The Journal of Physical Chemistry. B 110 (2006) 2833.
[12] C.G. Hanke, S.L. Price, R.M. Lynden-Bell, Molecular Physics 99 (2001) 801.
[13] C.J. Margulis, H.A. Stern, B.J. Berne, The Journal of Physical Chemistry. B 106 (2002) 12017.
[14] Y. Wang, W. Jiang, T. Yan, G.A. Voth, Accounts of Chemical Research 40 (2007) 1193.
[15] T.J. Gannon, G. Law, P.R. Watson, Langmuir 15 (1999) 8429.
[16] G. Law, P.R. Watson, Langmuir 17 (2001) 6138.
[17] G. Law, P.R. Watson, Chemical Physics Letters 345 (2001) 1.
[18] G. Law, P.R. Watson, A.J. Carmichael, K.R. Seddon, Physical Chemistry Chemical Physics 3 (2001) 2879.
[19] S.J. Baldelli, The Journal of Physical Chemistry. B 107 (2003) 6148.
[20] S. Rivera-Rubero, Journal of the American Chemical Society 126 (2004) 11788.
[21] K.A. Fletcher, S. Pandey, Langmuir 20 (2004) 33.
[22] J. Bowers, C.P. Butts, P.J. Martin, M.C. Vergara-Gutierrez, R.K. Heenan, Langmuir 20 (2004) 2191.
[23] J. Bowers, M.C. Vergara-Gutierrez, J.R.P. Webster, Langmuir 20 (2004) 309.
[24] J. Sung, Y. Jeon, D. Kim, T. Iwahashi, T. Iomori, K. Seki, Y. Ouchi, Chemical Physics Letters 406 (2005) 495.
[25] T. Iimori, T. Iwahashi, H. Ishii, K. Seki, Y. Ouchi, R. Ozawa, H. Hamaguchi, D. Kim, Chemical Physics Letters 389 (2004) 321.

[26] E. Solutskin, B.M. Ocko, L. Taman, I. Kuzmenko, T. Gog, M.J. Deutsch, Journal of the American Chemical Society 127 (2005) 7796.
[27] V. Halka, R. Tsekov, W. Freyland, Physical Chemistry Chemical Physics 7 (2005) 2038.
[28] T.Y. Yan, C.J. Burnham, M.G.D. Pópolo, G.A. Voth, Journal of Physical Chemistry. B 108 (2002) 11877.
[29] R.M. Lynden-Bell, Molecular Physics 101 (2003) 2625.
[30] R.M. Lynden-Bell, J. Kohanoff, M.G.D. Pópolo, Faraday Discussions 129 (2005) 57.
[31] R.M. Lynden-Bell, M.G.D. Pópolo, T.G.A. Youngs, J. Kohanoff, C.G. Hanke, J.B. Harper, C.C. Pinilla, Accounts of Chemical Research 40 (2007) 1138.
[32] J. Picálek, B. Minofar, J. Kolafa, P. Jungwirth, Physical Chemistry Chemical Physics 10 (2008) 5765.
[33] T.M. Chang, L.X. Dang, Journal of Physical Chemistry. A 113 (2009) 2127.
[34] L.X. Dang, Journal of Chemical Physics 97 (1992) 2659.
[35] D.H. Herce, L. Perera, T.A. Darden, C. Sagui, Journal of Chemical Physics 122 (2005) 24513.
[36] H.J.C. Berendsen, D. van der Spoel, R. van Drunen, Computer Physics Communications 91 (1995) 43.
[37] E. Lindahl, B. Hess, D. van der Spoel, Journal of molecular modeling 7 (2001) 306.
[38] A.W. Schuettelkope, D.M.F. van Aalten, Acta Crystallographica D60 (2004) 1355.
[39] R.M. Lynden-Bell, T.G.A. Youngs, Journal of Physics: Condensed Matter 21 (2009) 424120.
[40] T. Yan, J. Burnham, M.G.D. Pópolo, G.A. Voth, The Journal of Physical Chemistry. B 108 (2004) 11877.
[41] T.M. Nymand, P. Linse, The Journal of Chemical Physics 112 (2000) 6152.
[42] I.C. Yeh, M.L. Berkowitz, The Journal of Chemical Physics 111 (1999) 3155.
[43] A. Toukmaji, C. Sagui, J. Board, T. Darden, The Journal of Chemical Physics 113 (2000) 10913.
[44] D.J. Lyttle, J.R. Lu, T.J. Su, R.K. Thomas, J. Penfold, Langmuir 11 (1995) 1001.
[45] M. Tarek, D.J. Tobias, M.L. Klein, The Journal of Physical Chemistry 99 (1995) 1393.
[46] M. Mucha, T. Frigato, L.M. Levering, H.C. Allen, D.J. Tobias, L.X. Dang, P. Jungwirth, The Journal of Physical Chemistry. B 109 (2005) 7617.
[47] P.B. Petersen, R.J. Saykally, M. Mucha, P. Jungwirth, The Journal of Physical Chemistry. B 109 (2005) 10915.
[48] P.C. Hiemenz, R. Rajagopalan, Principles of Colloid and Surface Chemistry, Marcel Dekker, Inc., New York, third edition, pp. 343–348.
[49] W. Jiang, Y. Wang, G.A. Voth, The Journal of Physical Chemistry. B 111 (2007) 4812.
[50] D.J.V.A. dos Santos, F. Müller-Plathe, V.C. Weiss, The Journal of Physical Chemistry. C 112 (2008) 19431.